OPTICAL DESIGN WITH THE SCHMIDT CONCEPT

1. GROUND-BASED DEVELOPMENT
2. THE SPACE SCHMIDT PROJECT FOR THE 1990'S ?

G. Lemaître

Observatoire de Marseille
Place Le Verrier, 13248 Marseille, France

The basic principle of the camera described by Bernard Schmidt in 1932 is that a single concave mirror with a stop at its center of curvature has no unique axis and therefore yields equally good images at all points of its yield. The field is curved, and to correct the spherical aberration produced by the mirror, Schmidt introduced, in the stop at the center of curvature of the mirror, a thin non spherical corrector plate of glass. Around 1930 at the Hamburg Observatory and in spite of many difficulties, it was Schmidt's genius as an optician that succeeded - after several judiciously interpreted trials - in figuring a corrector plate by elastic relaxation, and thus demonstrated the optical performance of this new generation of instruments.

For such critical photographic work as sky surveys by the Palomar, ESO and UK Schmidt telescopes, an attempt was made to match the size of the residual aberrations to that of the resolving power of the emulsion used. A third order theory has been treated by Strömgren (1935) for minimizing the chromatism, by Carathéodory (1940) for the determination of the on-axis stigmatism and by Linfoot (1949) for the optimization and balancing of the aberrations in the field. The theory of elasticity applied to the original Schmidt method of figuring aspherical plates has been treated by Couder (1940).

The length of a Schmidt telescope is twice that of the focal length. At low F-ratio the concave mirror would be much larger than the corrector plate and the length of the telescope prohibitive. Ratios between F 2.7 and F 3.5 were mainly adopted for large classic (refractive) singlet corrector Schmidt, but it has been shown that the chromatism of even a fused silica plate hardly limits the optical performance of the system. Solutions for reducing this effect will be presented below. New developments, such as all-reflective design and spectrographic cameras using aspherical reflective gratings, need the treatment of a more elaborate theory of aberrations than the third order one. New methods of figuring refractive or reflective corrector, and aspherical gratings by elastic relaxation are very efficient if used with plane polishing.

M. Capaccioli (ed.), Astronomy with Schmidt-Type Telescopes, 533–548.

1. GENERAL DESIGN

A large variety of systems can be designed according to the principle outlined by Schmidt of locating both the stop and the corrector at the center of curvature C of the mirror. This is the case with refractive or, more recently reflective cameras working with object at infinity or at a finite distance and also new spectrographic cameras using aspherical reflective gratings.

1.1 WAVEFRONT FIGURES AT THE CENTER OF CURVATURE OF A SPHERICAL MIRROR

For determining the correction to be done in C with corrective element, let us consider, as in Figure 1, a point source I that will become the stigmatic image point of the system with the corrector. The shape of the corrective element can be readily defined from that of the wavefront $Z_w(r)$ passing point C after reflection at P on the mirror whose radius of curvature is R. The Gaussian focus G of the mirror alone for an object at infinity is located midway between segment CS. Let GI = M x R/2 be the distance from the point source I to the point G. The adimensional parameter M is not necessarily small and takes any negative values between 0 and - 1 for Schmidt cameras working at finite distance, as is shown in the case of Figure 1. With the object at infinity, M is positive and relatively small, and point I is close to point G - between G and S.

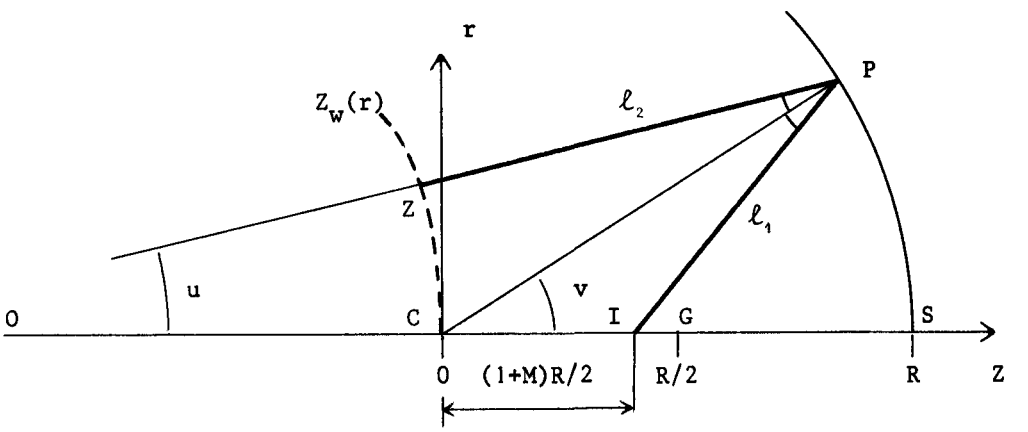

Figure 1. Reflection at a spherical mirror.

The shape of the wavefront $Z_w(r)$ can be obtained from the condition of a constant light path 2 IS + IC on the axis, so that for a point P of the mirror and for positive lengths IP = ℓ_1 and PZ = ℓ_2

$$\ell_1 + \ell_2 = (3 - M)R/2 \qquad (1)$$

In a cylindrical coordinate system the wavefront $Z_w(r)$ can be expressed

https://doi.org/10.1017/S025292110010716X Published online by Cambridge University Press

by the even polynomial series

$$Z_w = \sum_{n=1} A_{2n} \, r^{2n}/R^{2n-1} \qquad (2)$$

For large spectrographic cameras having an F-ratio as fast as F1, high order terms of eq. (2) will be necessary to obtain an accurate correction and also as starting parameters for solving the elasticity problem, mainly in the case of aspherical gratings - working at infinity - where deformable masters, used for replication, are free of the thickness distribution.

A set of relations can be deduced from the geometrical properties of Figure 1, where u and v are respectively the angles of segments ZP and CP with the Z axis. These are

$$\begin{aligned} Z_w &= R \cos v - \ell_2 \cos u \\ r &= R \sin v - \ell_2 \sin u \\ \ell_1 \cos u &= R \cos v - (1+M) R/2 \\ \ell_1^2/R^2 &= (5 + 2M + M^2)/4 - (1+M) \cos v \end{aligned} \qquad (3)$$

An extremely laborious work using numerous series expansions and many operation on these has been carried out from relations (1) and (3) for the determination by identification with the coefficients A_{2n} of eq. (2). This analysis would be too long to be presented here but could be published later. For the five first coefficients, the result is

$$A_2 = \frac{M}{1+M}, \qquad A_4 = -\frac{1}{4} \frac{1 - M - M^2 - 3M^3}{(1+M)^3} \qquad (4)$$

$$A_6 = -\frac{3}{8} + 2M - 4M^2 + \ldots, \quad A_8 = -\frac{45}{64} + 4M - \ldots, \quad A_{10} = -\frac{193}{128} + \ldots,$$

In the case of a camera working with an object at finite distance, the adimensional parameter M is also the magnification ratio, i.e. $M = -CI/CO = -SI/SO$. As a verification, the first two coefficients of relations (4) give a spherical wavefront for the particular cases where $M = +1$ and $M = -1$, corresponding respectively to point I in S and point I in C.

1.2 WAVEFRONT FIGURE FOR AN OBJECT AT INFINITY

In this section and the following, only the case of object at infinity is to be considered so that the point I is close to G. For I at G, parameter $M = 0$ and coefficient $A_2 = 0$; the aspherical wavefront does not presents curvature in C. When optimizing the corrector for reducing off-axis aberrations and possibly on-axis sphero-chromatism for refractive elements, one will need a coefficient A_2 of sign opposite to that of the higher coefficients. These wavefronts shows an inflexion point, and for a radial distance r_o the propagation is parallel to the Z axis. If r_m is the radius of the clear aperture beam, the zone of parallel

https://doi.org/10.1017/S025292110010716X Published online by Cambridge University Press

propagation can be characterized by a a ratio as

$$a = r_o^2/r_m^2 \tag{5}$$

The ratio is defined by $F = R/2r_m$, since parameter M is necessarily small. From the derivation of the two first terms in eq. (2), one obtains as a first approximation

$$M \simeq a/2^5F^2 \tag{6}$$

For a = 1, the wavefront is parallel to the Z axis for $r_o = r_m$. As will see, optical optimizations lead us mainly to study cases where $a < 1$ and $a > 1$.

1.3 DESIGN OF VARIOUS CORRECTIVE ELEMENTS

Refractive or reflective correctors and self-corrective gratings can be used in Schmidt's design. To avoid full obstruction of the camera, a tilt of the corrector is necessary if there is a reflection. Let us consider a cylindrical coordinate system Z, r, θ, linked to the corrector, with the r, θ plane being tangent to it at its vertex C, the Z axis being positive toward the spherical mirror and θ = 0 in the symmetry plane of the camera. The general figure $Z(r,\theta)$ of the corrective element is of the form

$$Z = \Sigma\, B_{m,2n}\, r^{2n} \cos m\theta / R^{2n-1}, \tag{7}$$

and will be defined from that of the wavefront Z_w as defined in eq. (2) and (4) by the following relation

$$B_{m,2n} = s\,\mu\, T_{m,2n} \cdot A_{2n}\ , \tag{8}$$

where s is a field optimization factor very close to unity (see below), μ is a constant depending upon the mounting and the nature of the corrector and $T_{m,2n}$ are coefficient appearing for tilted correctors. Table 1 lists the values of μ and ratios $B_{m,2n}/A_{2n}$ for different types of corrector. For a refractive plate the rays are assumed to emerge from the aspherical surface that faces the concave mirror. The case where the reflective corrector is not tilted leads to full obstruction on-axis but can be usable off-axis. This family belongs to the class of centred systems. The case where the reflective corrector is tilted by an angle i has been listed with $t = \frac{1}{2}\sin^2 i$. This is also valid for Littrow-mounted reflective gratings.These families belong to the class of non-centred systems : the figure of the corrector is of bi-axial symmetry. For spectrographs, self-corrected reflective gratings have a rotational symmetry if mounted in normal diffraction (β = 0).

At the edge of the field, 1) the corrective element gives a stronger correction than when working on-axis. This being due to the inclination φ of the incident beams, and 2) the stop is circular but

https://doi.org/10.1017/S025292110010716X Published online by Cambridge University Press

the cross-section of the off-axis beams is elliptical. Thus the corrective element increases the correction in the sagital section of these beams. This two off-axis effects produce degradation of the astigmatism type. For field optimization it is necessary to choose, if possible, an s value slightly under unity to under-correct the aspherical element.

TABLE 1. Value of μ and $B_{m,2n}/A_{2n}$ for different types of corrector

CORRECTOR TYPE	REFRACTIVE PLATES Correcting for index n	REFLECTIVE MIRRORS without tilt, 100% obstruction on-axis	REFLECTIVE MIRRORS OR GRATINGS IN LITTROW tilt angle = i	REFLECTIVE GRATINGS incident angle = α diffraction angle $\beta = 0$
μ	$-1/(n-1)$	$1/2$	$1/2 \cos i$	$1/(1+\cos\alpha)$
$B_{0,2}/A_2$	$-s/(n-1)$	$s/2$	$s(1-t)/2 \cos i$	$s/(1+\cos\alpha)$
$B_{2,2}/A_2$	0	0	$-st/2 \cos i$	0
$B_{0,4}/A_4$	$-s/(n-1)$	$s/2$	$s(1-2t+\frac{3}{2}t^2)/2 \cos i$	$s/(1+\cos\alpha)$
$B_{2,4}/A_4$	0	0	$-2st(1-t)/2 \cos i$	0
$B_{0,6}/A_6$	$-s/(n-1)$	$s/2$	$s(1-3t)/2 \cos i$	$s/(1+\cos\alpha)$

2. REFRACTIVE CAMERAS

2.1 OFF-AXIS ABERRATIONS AND CHROMATISM OF A SINGLET PLATE

To determine the size of off-axis images at an angle φ from the axis, spot diagrams have been obtained with 73 rays in the stop. There are 1, 16, 24 and 32 rays for semi-apertures of 0, $r_m/2$, $3\,r_m/4$ and r_m, respectively, (see Figure 2 at the top of the curves). First, different values of the parameter M, and then a from eq. (6), are considered with s = 1. Off-axis images are plotted on the sphere of center C and radius $(1+M)R/2$ that gives the on-axis stigmatism. The two-dimensional size of these images is denoted by ℓ_r and ℓ_t, in the radial and tangential directions respectively. These spot-diagrams are shown at the top line of Figure 2, the center of the field being in the vertical direction of the Figure. Except for a = 4/3, these images can be improved by focusing by the quantity Δf. The sign of Δf is positive for a focusing toward the mirror. One then obtains images inscribed in a circle of minimum diameter d. These spot diagrams are shown on the second line of Figure 2. Variations of the quantities ℓ_r, ℓ_t, d and Δf with the parameter a are given as a function of the quantities F, φ

https://doi.org/10.1017/S025292110010716X Published online by Cambridge University Press

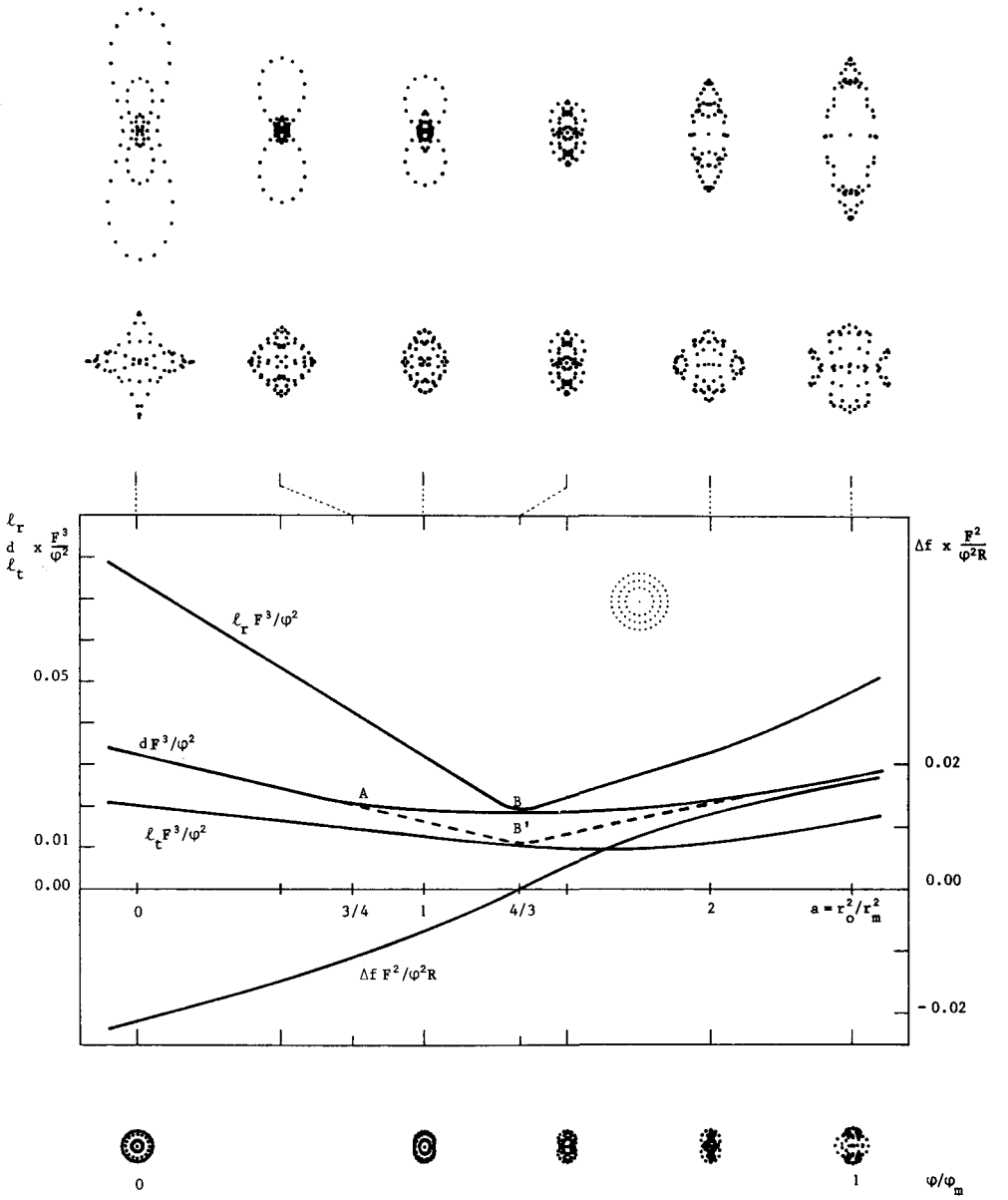

Figure 2. Off-axis residual aberrations of refractive Schmidts

https://doi.org/10.1017/S025292110010716X Published online by Cambridge University Press

and R. As results, for a = 3/4, i.e. a null power zone at $r_o = 0.866\ r_m$, the diameter of the largest image is

$$d = 0.020\ \varphi^2/F^3$$
$$s = 1, \quad a = 3/4 \quad \text{i.e.} \quad M = 3/128\ F^2 \tag{9}$$

(cf. point A, Fig. 2). For a = 4/3 the null power zone is at $r_o = 1.155\ r_m$, out of the clear aperture and $d = 0.0185\ \varphi^2/F^3$ (cf. point B, Fig. 2)which is the minimum for s = 1.

In the range $1 < a < 5/2$ it is possible to improve the resolution by undercorrecting the plate. If φ_m is the semi-field angle to optimize, the best parameter of under-correction is $s = \cos^2 \varphi_m$. After focusing, the size of the off-axis blur at $\varphi = \varphi_m$ is shown by the dotted-line of Figure 2. The best resolution is again for a = 4/3 (cf. point B', Fig. 2)

$$d = 0.011\ \varphi_m^2/F^3$$
$$s = \cos^2 \varphi_m, \quad a = 4/3 \quad \text{i.e.} \quad M = 1/24\ F^2 \tag{10}$$

Spot-diagrams of this optimization are shown on a spherical surface for different field values φ/φ_m at the bottom line of Figure 2. For instance, at F3 and for $2\varphi_m = 5°$ the diameter of the images according to eq. (9) and (10) do not exceed 0.29 and 0.16 arcsec respectively.

Unfortunately, for singlet refractive plates, the chromatic variation of spherical aberration is much larger than off-axis aberrations. To minimize the effect of this variation, the slope of the correcting plate must be chosen as weak as possible in absolute value. This criterium,which corresponds to the old rule stated by Kerber in 1886 to optimize blue and red wavelengths of composite lenses, is translated here by a = 3/4, giving a correcting plate having opposite slopes at $r_o = r_m/2$ and $r_o = r_m$. If the plate is designed for correcting the wavelength λ_o with refractive index n_o (on-axis stigmatism), at the wavelength λ with n as the corresponding refractive index, the angular diameter of the on—axis image (c.f. Bowen, 1960) is

$$d_\lambda = 1/128\ F^3\ \nu \tag{11}$$

where $\nu = (n_o - 1)/(n_o - n)$. For an F3 telescope and a plate in fixed silica correcting for $\lambda_o = 405$ nm, at $\lambda = 320$ nm or at $\lambda = 656$ nm the absolute value of ν is $\nu = 36$ and eq. (11) gives $d_\lambda = 1.6$ arcsec.

Finally if d_φ is the diameter on off-axis image given by eq. (9) and d_τ that of the seeing, the image size in the field of a singlet plate Schmidt cannot be better than

$$D < d_\varphi + d_\lambda + d_\tau = 20\ 10^{-3}\ \varphi^2/F^3 + 7.8\ 10^{-3}/F^3\nu + d_\tau \tag{12}$$

If d_τ is 1 arcsec, singlet plate Schmidts designed at F3 with $2\varphi = 5°$ in the wavelength range 320 - 656 nm have residual aberrations of at least 3 arcsec. Improving this resolution by factor 2 would lead in

https://doi.org/10.1017/S025292110010716X Published online by Cambridge University Press

the same conditions to an aperture of F 4.75 and then a very long tube.

2.2 ADDITION OF A MENISCUS FOR CORRECTING THE RED REGION

The predominant effect of the sphero-chromatic aberration of a singlet corrector plate can be divided by a factor two by adding a meniscus just before the focus only when working in the red region of the spectrum. The full spectral range of the telescope is then shared by blue and red, each range corresponding to an equal variation Δn of the refractive index of the plate. The plate is designed alone with $a = 3/4$ for correcting the blue; this gives an under-correction in the red which is compensated by adding a monocentric meniscus. Both mirror and meniscus have a common center of curvature so that no off-axis aberrations are added by the meniscus. If N is its mean index in the red, its thickness is roughly equal to

$$e = \frac{1}{8} \frac{\Delta n}{n-1} \frac{N^3}{N^2-1} R \qquad (13)$$

The image size in the field for this design is given in eq. (12) where now the number ν is twice as great as for the singlet plate of the previous section if the full spectral ranges (red + blue) are the same. For instance, an F3 telescope of 1 meter clear aperture having a plate and a meniscus in fused silica and extended spectral range such as 320 to 440 nm in the blue and 440 to 1000 nm in the red leads to a meniscus of 65 mm thickness.

An inconvenience of this design is to use two plate-holders of slightly different curvature and collimation. The red plate scale is smaller than that of the blue plate (0.8% smaller for the preceding example). Advantages of this solution (compared to that described in following section) are the high transparency of a singlet plate in the UV and also of having only one aspherical surface to figure. Also, filters can be inserted into the meniscus for cutting off the shorter wavelengths without additional glass-air surfaces.

2.3 DOUBLET PLATE CORRECTOR

Another possibility for correcting the sphero-chromatism aberration of a single plate is to design a doublet plate corrector. If λ and λ' are the two wavelengths for which the instrument is corrected and n and n' the refractive indices, one can define the number $\nu = (n_o - 1)/(n - n')$ for each glass as ν_1 and ν_2. Let us suppose that ν_2 corresponds to the most dispersive glass. If ψ_1 and ψ_2 are the powers of the plates for a given value of the a ratio, and ψ that of a singlet plate correcting for index n_o, the condition of a chromatism is

$$\psi_1/\nu_1 + \psi_2/\nu_2 = 0 \quad \text{and} \quad \psi_1 + \psi_2 = \psi \qquad (14)$$

giving the power of the components as

$$\psi_1 = \frac{\nu_1}{\nu_1 - \nu_2} \psi \quad \text{and} \quad \psi_2 = \frac{-\nu_2}{\nu_1 - \nu_2} \psi, \qquad (15)$$

https://doi.org/10.1017/S025292110010716X Published online by Cambridge University Press

the correcting plate of most dispersive glass being divergent. Assuming that the secondary chromatism is negligeable, one can choose the ratio a = 4/3 for a better off-axis correction of the two plates (cf. resolution given by eq. (10)), and then the null power zones are out of the clear aperture. The figure of the two plates can be written by using the parameter s of eq. (8) as

$$s_1 = \frac{\nu_1}{\nu_1 - \nu_2} \cos^2 \varphi_m \quad \text{and} \quad s_2 = - \frac{\nu_2}{\nu_1 - \nu_2} \cos^2 \varphi_m \ . \qquad (16)$$

For instance a Schmidt at F3 achromatized at λ = 365 nm and λ' = 588 nm by using Schott glass like crown UBK7 ($\nu_1 \simeq 27$) and light flint LLF1 ($\nu_2 \simeq 18$) have plates of equivalent asphericity of F2.06 for the crown and of F2.35 for the flint which is divergent at its vertex. Such correcting plates were built for the 1.2 m, F3 UK Schmidt in Siding Spring (Australia) while another doublet is under completion for the 1 m, F3 ESO Schmidt in La Silla (Chile).

3. REFLECTIVE TELESCOPES

All-reflecting Schmidts are particularly well adapted for carrying out sky surveys from space (Fig. 3). Below, optical performance will be compared between centred systems working off-axis and non centred systems. The best result is in favour of the latter.

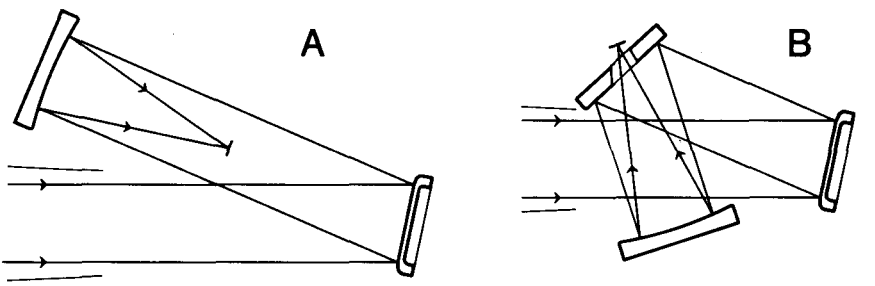

Figure 3. Reflective Schmidts

3.1 CENTRED SYSTEMS OPTIMIZED OFF-AXIS

Let us consider, first, a full obstructed centred system. As was done for refractive telescopes, and for a parameter s = 1, off-axis images have been plotted, as a function of the a ratio, on the sphere of center C and radius (1 + M)R/2 that gives the on-axis stigmatism. The size of these images is denoted by ℓ_r out ℓ_t in the radial and tangential directions respectively (see spot-diagrams at the top line of Fig. 3). With the same conventions as for § 2.1 the diameter of the best images d and defocussing Δf are also given for the spot-diagrams on the second line of Figure 4. The result is that for a = 3/2, i.e. a

https://doi.org/10.1017/S025292110010716X Published online by Cambridge University Press

null power zone at $r_o = 1.22\ r_m$, the diameter of the off-axis blur is close to the minimum. A careful interpolation between the considered values of a seems to give the smallest blur for $r_o = 1.10\ r_m$, which corresponds to $a = \sqrt{2}$. If φ_m is the semi-field angle to be optimized, the best parameter of under-correction is $s = \cos \varphi_m$. After focussing, the size of the off-axis blur at $\varphi = \varphi_m$ is shown by the dotted line of Figure 4. For a = 3/2 the best resolution is $d = 0.011\ \varphi_m^2/F^3$. Spot-diagrams of this optimization are shown on a spherical surface for different field values φ/φ_m on the bottom line of Figure 4.

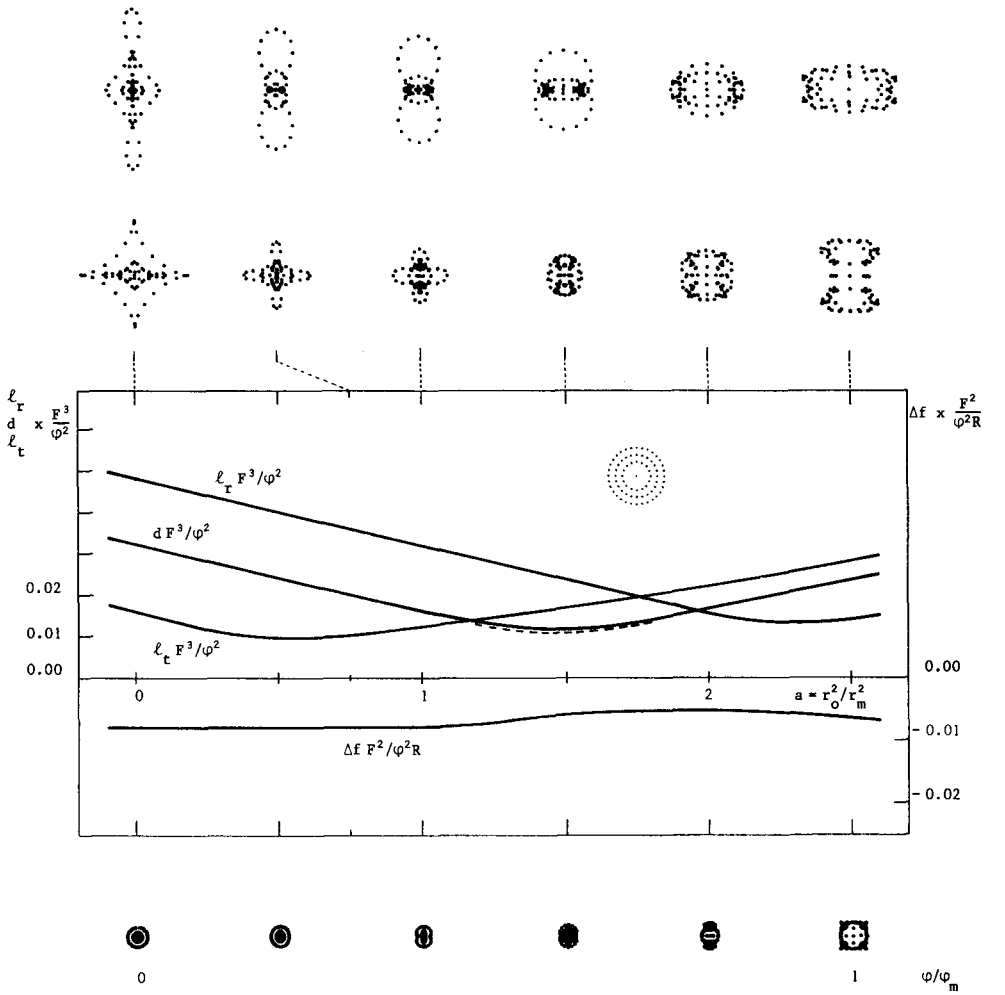

Figure 4. Off-axis residual aberrations of centred reflective Schmidts

To make such a two-reflection telescope practicable and then avoid the obstruction, the angle of incidence of the principal beam must be

https://doi.org/10.1017/S025292110010716X Published online by Cambridge University Press

at least

$$i = \varphi_m + 1/4\ F \qquad (17\text{-}1)$$

When adding a holed folding mirror (three-reflection telescope) for a better detector access to the focus, this angle can be kept as

$$i = \varphi_m + 7/16\ F \qquad (17\text{-}2)$$

Relations (17-1) and (17-2) hold for beams having circular cross-section. For both of the preceding mountings, the resolution for the most off-axis beam of inclination $i + \varphi_m$ is

$$d_c = 0.011\ (i+\varphi_m)^2/F^3 \qquad (18)$$
$$s = \cos\ (i+\varphi_m)\ , \quad a = 3/2 \quad \text{i.e.} \quad M = 3/64\ F^2$$

This resolution is the same as that found for a monochromatic refractive camera (cf. eq. (10)).

3.2 NON CENTRED SYSTEMS

For a non-centred system the mounting is the same as for the preceding section. Relations (17) hold , but the shape of the correcting mirror is not a surface of revolution. The level lines of this surface are homothetical ellipses as defined by eq. (7) and (8) and coefficients given in the forth column of Table 1, so that stigmatism is achieved at the center of the field.

The best resolution is again determined by ray tracing with respect to the a ratio. The result is that the null power zone is slightly under a = 3/2 as for the preceding section. An under-correction of the corrector does not improve the performance. For the two points at the edge of the field and in the symmetry plane of the telescope, the largest blur is that which corresponds to the largest distance from the Z axis of the corrector. The angular diameter of that image is found as

$$d_{NC} = 0.012\ \varphi_m\ (\tfrac{3}{2}\ i + \varphi_m)/F^3 \qquad (19)$$
$$s = 1\ , \quad a = 3/2$$

Figure 5 gives spot diagrams in the field of a design with a = 1. For this ratio the image blurs are 1.44 times larger than for eq. (19) but the corrector can be readily figured by the elastic relaxation technique using a built-in edge at the null power zone.

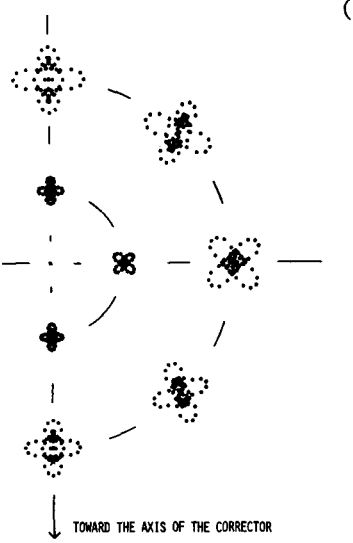

Figure 5. Off-axis residual aberrations in the field of non-centred reflective Schmidts for a = 1

https://doi.org/10.1017/S025292110010716X Published online by Cambridge University Press

3.3 GAIN OF NON-CENTRED SCHMIDTS

For an image-blur having larger size than that of the detector pixel the gain in magnitude of the non-centred design over the centred system is readily determine from eq. (18) and (19). Considering with eq. (17-2) the folded three-reflection design, one obtains

$$\Delta m = 2.5 \log (d_C^2/d_{NC}^2) = 5 \log \frac{11}{18} \frac{(2\varphi_m + 7/16\,F)^2}{\varphi_m(\varphi_m + 7/16\,F)} \qquad (20)$$

As instance, at F3 with a semi-field $\varphi_m = 2.5°$, the gain in magnitude is $\Delta m = 2.7$, and the non-centred design gives, at the edge of the field, an image blur equal or smaller to 1.2 arcsec (G. Lemaître, 1976, 1979, 1980). This performance is very promising for carrying-out the construction of a 2 meter focal length space Schmidt telescope for an UV Survey. Proposals submitted to NASA (J. Wray et al., 1982) could be retained in the future.

4. SCHMIDT SPECTROGRAPHS WITH REFLECTIVE ASPHERICAL GRATINGS.

In a slit spectrograph using reflective gratings, one of the difficulties encountered is the obstruction of the incident beam by the camera optics. To avoid this, the camera optics are usually designed to be placed at a distance of several times the collimator diameter from the gratings. It is then necessary to provide camera optics having an aperture substantially larger than that of the collimator beam if severe losses due to vignetting are to be avoided at the edges of spectra. These optics, much larger than the grating size,have increased asphericities, and for cameras of fast F ratios the figuring of such optics becomes crucial.

Aspherical gratings have been produced by the elastic relaxation method These gratings lead to more nearly ideal mountings from the standpoints of a small number of surfaces, of a fast F ratio and of a wide field. An example of the procedure is the following. 1) A plane grating is duplicated on a flexible optical blank when in a state of zero stress. 2) The flexible blank is re-duplicated while submitted to a state of stress giving the required asphericity by flexure.

Four arrangements having the same focal length, F ratio and field of view are shown in figure 6. The first mounting is obtained with a classical refractive schmidt camera (a). In (b) a doublet corrector camera is used with all surfaces spherical and one type of glass. The doublet corrector can be replaced by a Maksutov or a Bouwers meniscus, but the optical positioning is kept approximately identical. One method of avoiding the difficulty of these large correctors is to place the corrector parallel to the grating and practically in contact

with it (Bowen, 1952). The light then passes the corrector plate twice, once before and once after diffraction at the grating (c). It can be shown that in this case, the figure of the twice-trough plate is reduced by the factor $(1+\cos\alpha)/\cos\alpha$ from that of the regular once-through plate (a), where α is the angle of incidence on the plate and the grating. The chromatic aberrations are essentially the same as for the conventional corrector plate. With aspherical gratings (Lemaître, 1977) these chromatic aberrations are entirely suppressed and the problem of four refrac tions in (c) vanishes. Table 1 shows that for mountings (d) the figure of the corrective grating is reduced by the factor $(1+\cos\alpha)/(n-1)$ from that of the regular once through plate (a). For a grating having symmetry of revolution the axis of the camera is taken nearly normal to the grating ($\beta=0$). The coefficients defining the figure of the grating according to eqs (7) and (8) are given in the fifth column of Table 1. The residual off-axis aberrations are smaller than those given by eq. (18) for centred reflective Schmidts in which the angle i is taken equal to zero.

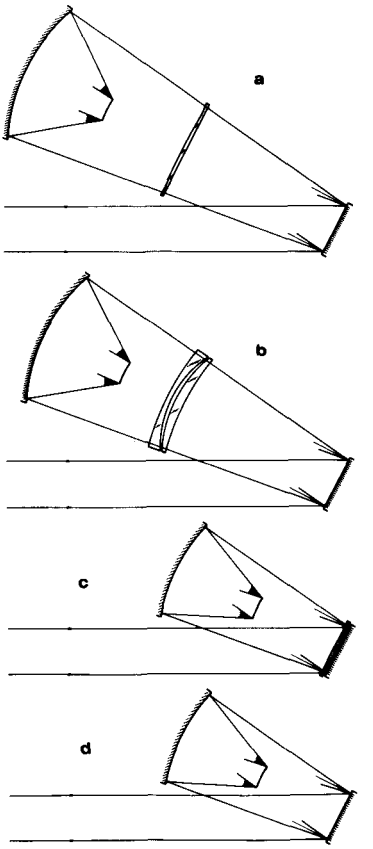

Fig.6 - Comparison of four spectrographic mountings using the same reflective grating.

The reflective normal diffraction mounting is surely the highest performance design of all those based on the Schmidt concept. For cases where the angle of diffraction β is non-zero , such grating have only a bi-axial symmetry, as for the Littrow mount, the aspherical coefficients of which, are given in the fourth column of Table 1. In order to obtain a more accessible focus, folding mirrors have been placed between the gratings and the camera mirror. These holed mirrors can fold either both incident and diffracted beams, or only the latter.

https://doi.org/10.1017/S025292110010716X Published online by Cambridge University Press

5. TRENDS FOR SCHMIDTS IN ASTRONOMY

Because of their wide field of view, Schmidt cameras have found many uses in astronomy (detection, identification, classification). The main optical designs are the followings :

- photography for sky surveys and selected areas.
- field spectrography with single prisms.
- field spectrography with a two position bi-prism for measuring the radial velocities of stars and nebulas. An accuracy of 4 km/s is obtained (Fehrenbach, 1981).
- Schmidt cameras and their modifications especially for slit spectrographs on large telescopes.

Ground-based Schmidt telescopes are susceptible to differential refraction effects in the field. For this reason, larger field Schmidts could be built only if the size of the corrector were increased and the focal length kept not very different than usual in order to decrease the exposure time. Critical definition of such refractive Schmidts, as given in section 2 by eq. 10, is valid only for a doublet lens corrector having a null secondary chromatism. Under this assumption a Schmidt at F2.2 will have a fifth order astigmatism blur of 1 arcsec at the edge of a field of 7.5° in diameter.

A space Schmidt telescope could surely bring more spectacular discoveries at a price of less optical research than those needed for a very large ground based Schmidt. In 1963, Henize proposed to NASA the use of a Schmidt telescope in space for an UV sky survey.

A two-mirror reflective Schmidt was presented by Epstein (1967) and a folded version was developped by Wray (1969). These were designed with the centred system concept used off-axis.

Fifth order astigmatism can be reduced by using non-centred systems e.g. tilted correctors that have bi-axial symmetry. Korsch (1974) and Lemaître (1976) have given the figure of such correctors for a zonal-ratio $a = 0$. Schroeder (1977) has improved the performance by taking $a = 3/4$. Optimization of the corrector zonal-ratio led finally to choose $\sqrt{2} < a < 3/2$ (Lemaître, 1979) for obtaining the best optical performance. For these values the null power zone is out of the clear aperture. The corresponding size of residual aberration is given in section 3.2 by eq. 19 and the gain over centred systems in section 3.3.

The folding mirror is holed, as for modern spectrographic cameras, in order to adapt a large curved cathode detector. Cathodes of 10 cm in

diameter are now in operation in different observatories and have a resolution better than 10 μm with a permanent magnet focussing. A 20 cm detector as needed for the space Schmidt can readily be made (Carruthers, 1979 ; Griboval, 1983 ; Servan, 1983) but the cost is not negligeable for working with an automatic film transport.

At F 3.2 with a 5° field, a resolution of 1 arcsec is achieved. The feasibility of such a complete instrument has been demonstrated and has led, for its construction, to the proposed joint American-Italian-French Schmidt Telescope Project (Wray, 1982).

the S S T in the 90's
will be surely for the S T
a good fellow

REFERENCES

Bowen, I.S.: 1952, *Ap. J.* 116, 1.
1960, *Telescopes, Stars and Stellar Systems*, Vol. I, ed. Kuiper, p. 58.
Caratheodory, C.: 1940, Hamburg. Math. Einzelschr., 28.
Carruthers, G.R.: 1979, *Advances in Electronics and Electron Physics*, 52, 283.
Couder, A.: 1940, *Comptes-Rendus*, Paris, 210, 327.
Epstein, L.C.: 1967, *Publ. Astron. Soc. Pacific*, 79, 132.
Fehrenbach, C., Burnage, R.: 1981, *Astron. Astrophys. Suppl. Series*, 43, 297.
Griboval, P.: see this Colloquium.
Henize, K.G.: 1963, *NASA Proposal*, Northwestern Univ.
Kerber, see in Chretien, H.: 1958, *Le Calcul des Combinaisons Optiques*, Ed. Sennas, Paris, 346.
Korsch, D.: 1974, *Appl. Optics*, 13, 2005.
Lemaître, G.: 1976, *J. Opt. Soc. Am.* 66, 12, 1334.
1977, *Astron. Astrophys.* 59, 249.
1979, *Comptes Rendus*, 288 B, 297.
1980, *Comptes Rendus*, 290 B, 171.
1981, *Current Trends in Optics*, ICO 12 Conference, Taylor et Francis, London 131.
Linfoot, E.H.: 1945, *Proc. Phys. Soc.*, London, 57, 209.
1949, *M.N.R.A.S.* 109, 279.
Linfoot, E.H., Wolf, E.: 1949, *J. Opt. Soc. Am.* 39, 752.

https://doi.org/10.1017/S025292110010716X Published online by Cambridge University Press

Schmidt, B.: 1932, Mitt. Hamburger Sternw., Bergedorf, 7, 36, 15.
Schroeder, D.J.: 1977, *Appl. Optics*, 17, 141.
Servan, B.: 1976, *IAU Colloquium n° 40*, Paris, 1.
Stromgren, B.: 1935, Vierteljahrsschr. Astr. Gessellsch., 70, 65.
Wray, J.D., O'Callaghan, F.G.: 1969, SPIE, Santa Barbara.
Wray, J.D., Smith, H.J., Henize, K.G., Carruthers, G.R.: 1982, SPIE, 332, 141.

https://doi.org/10.1017/S025292110010716X Published online by Cambridge University Press